

Analytical Methods

Accepted Manuscript



This is an *Accepted Manuscript*, which has been through the Royal Society of Chemistry peer review process and has been accepted for publication.

Accepted Manuscripts are published online shortly after acceptance, before technical editing, formatting and proof reading. Using this free service, authors can make their results available to the community, in citable form, before we publish the edited article. We will replace this *Accepted Manuscript* with the edited and formatted *Advance Article* as soon as it is available.

You can find more information about *Accepted Manuscripts* in the [Information for Authors](#).

Please note that technical editing may introduce minor changes to the text and/or graphics, which may alter content. The journal's standard [Terms & Conditions](#) and the [Ethical guidelines](#) still apply. In no event shall the Royal Society of Chemistry be held responsible for any errors or omissions in this *Accepted Manuscript* or any consequences arising from the use of any information it contains.

Theoretical use of boron nitride nanotubes as a perfect container for anticancer molecule

M. El Khalifi^a, E. Duverger^b, T. Gharbi^a, H. Boulahdour^a and F. Picaud^{a}.*

^aLaboratoire de Nanomédecine, Imagerie et Thérapeutique, Université Franche-Comté (UFR Sciences et Techniques), Centre Hospitalier Universitaire de Besançon, 16 route de Gray, 25030 Besançon, France

^b Institut FEMTO-ST, 32 Avenue de l'Observatoire, 25044 Besançon, France

*corresponding author email: fabien.picaud@univ-fcomte.fr Phone number: +33381666284

ABSTRACT

In recent years a great interest has emerged in the development of nanocarriers for drug transport. One of the major challenges is to obtain a drug delivery system able to control drug release profile, transport absorption and distribution, in a view of improving efficacy and safety. Herein, we present theoretical results based on density functional theory (DFT) to determine the best adsorption site of anticancer Ifosfamide molecule in boron nitride nanotube. For this functionalized system we determine the dependence of the adsorption energy on the displacement of molecules in the outer and inner boron nitride surfaces, together with their local morphological and charge modifications. Quantum simulations show that the most stable physisorption state is located inside the nanotube, with no net charge transfer between each subsystem, and no barrier

1
2
3 energy at the nanotube entrance. This demonstrates that chemotherapeutic encapsulation is the
4 most favorable way for Ifosfamide to be vectorized.
5
6
7

8
9
10 *Keywords:* boron nitride nanotubes; therapeutic agents; DFT calculations
11

12 13 **1. Introduction**

14
15 Nano-scale drug delivery systems are usually dedicated to target specific cells in tissues or
16 organs, and most of them are focused on cancer chemotherapy. Incorporating chemotherapeutics
17 drug in the accessible cavities of the nanocarriers and attaching receptors to the nanocarriers is
18 the most promising way to target precisely disease cells despite some drawbacks.¹⁻⁴ The
19 molecular size and the biodegradability of the nanocarrier are two very important factors since
20 the eventual nanocarrier clearance from the body, after delivering the drug, will depend on these
21 two parameters essentially. Nanotubes are very important geometric class of nanomaterials that
22 are used in biotechnology and medicine. Various types of drug/agent nanocarriers have been
23 investigated, among which a small number of such systems have been already commercialized or
24 are in clinical studies.⁵ In particular, carbon nanotubes (CNTs) have attracted a wide attention as
25 carriers for biologically relevant molecules, because of their unique physicochemical and
26 biological properties.^{4, 6, 7} Among all the nanocarriers studied, boron nitride nanotubes (BNNTs)
27 are structural analogues of CNTs nanomaterials. Their electrical properties are not dependent on
28 their chirality and diameter since they have a large band gap of about 5.5 eV.⁸ Their electrical
29 insulation is very high, despite a high thermal conductivity.⁹ Moreover, BNNTs have a high
30 hydrophobicity, a strong resistance to oxidation and to heat as well as a strong radiation
31 absorption resilience. Besides, they have been widely investigated in medical and biomedical
32 applications^{10, 11} after covalent or noncovalent functionalization of their outer surface to increase
33
34
35
36
37
38
39
40
41
42
43
44
45
46
47
48
49
50
51
52
53
54
55
56
57
58
59
60

1
2
3 their water dispersion.¹²⁻¹⁴ Density functional theory (DFT) studies have been conducted on the
4
5 noncovalent functionalization of BNNTs with benzaldehyde and seven different heterocyclic
6
7 aromatic molecules. They have shown that weak interactions give rise to new impurity states
8
9 within the band gap of pristine BNNTs suggesting the possibility of carrier doping through the
10
11 selective adsorption of aromatic rings.¹⁵ Moreover studies dealing with the interactions between
12
13 BNNTs and different molecules (azomethine (C₂H₅N), anticancer agent (Pt(IV)) complex linked
14
15 to an amino-derivative chain or Pt(IV) complex alone) have demonstrated the possibility to
16
17 obtain physisorbed or chemisorbed states. The most stable physisorption state was localized
18
19 inside the nanotube and the molecular chemisorption was possible above two adjacent B and N
20
21 atoms of a BNNT hexagon only. Note that the attachment of an azomethine plus a subsequent
22
23 drug did not perturb the cycloaddition process.¹⁶ Moreover, some preliminary applications in
24
25 biomedicine have emerged in the latest years showing no significant adverse effects for in vivo
26
27 study when BNNTs were injected in rabbits at a dose up to 10mg/kg. All these data suggested the
28
29 optimal biocompatibility of BNNTs, and thus open the way to their exploitation in
30
31 nanomedicine.^{17, 18} Ifosfamide (Ifos) is a cytotoxic anticancer chemotherapy drug belonging to
32
33 the category of mustard gas derivatives. It undergoes in the DNA formation and blocks the cell
34
35 replication without any selectivity for cancer cells, which implies a lot of secondary effects.
36
37 Driving the route of Ifos action using appropriate nanocarrier could definitively increase the
38
39 selectivity of the anticancer agent.
40
41
42
43
44
45
46
47

48 In this paper we report some new theoretical results concerning the adsorption of Ifosfamide
49
50 (Ifos) molecule on the outer and the inner BNNT nanocarrier surfaces. Thanks to full DFT
51
52 calculations, we investigate the energy behavior of Ifos molecule interacting with a BNNT
53
54 nanotube. We demonstrate that the molecule is able to encapsulate spontaneously and to find a
55
56
57
58
59
60

1
2
3 stable geometry leading to strong adsorption into the inner (10,10) BNNT sidewalls. To
4
5 demonstrate this, we investigated the energy stability of the functionalized systems through the
6
7 changes of their morphology and their electronic structure thanks to partial density of states
8
9 (PDOS) and Bader charge analysis.
10
11

12 2. Theoretical details

13
14 We studied system consisting of an armchair single-walled (10, 10) BNNT with finite-length
15
16 cylindrical BN cage (i.e. diameter radius 13.94 Å, length 21.32 Å), composed of 180 B and 180
17
18 N atoms. In order to avoid boundary effects, hydroxyl groups (–OH), consisting of 40 O and 40
19
20 H atoms, were introduced onto the BNNT extremities, as depicted in Fig. 1.¹⁴ BNNT nanotube
21
22 and Ifosfamide (C₇H₁₅Cl₂N₂O₂P) drug molecule were studied using the same unit cell (i.e. 50 x
23
24 50 x 60 Å³), where the last number represents the length of the unit cell along the tube axis.
25
26 Given the large unit cell, the Brillouin zone was sampled using a single k-point at the center Γ . A
27
28 basis set of localized atomic orbitals (double- ζ plus polarization functions), and norm-conserving
29
30 pseudopotentials were employed.
31
32
33
34
35

36
37 The adsorption energy (E_{ads}) of adsorbed molecules (Mol) on the inner surface of the BNNT
38
39 (Template) was derived from the energy difference between the different states of the system,
40
41 namely, $E_{\text{ads}} = E(\text{Mol} + \text{Template}) - E(\text{Template}) - E(\text{Mol})$. A negative E_{ads} value denoted a more
42
43 favorable interaction between the drug and the BNNT.
44
45

46
47 The total energies were obtained from *ab initio* calculations in the framework of Kohn-Sham
48
49 realization of the density functional theory DFT.^{19, 20} We used the Perdew-Burke-Ernzerhof
50
51 (PBE) generalized gradient approximation (GGA).²¹ for the exchange correlation density
52
53 functional as implemented in the SIESTA package.²² All calculations were performed without
54
55 spin polarization. We use the self-consistency mixing rate of 0.1, a maximum force tolerance of
56
57
58
59
60

0.01 eV/ Å and a mesh cut off of 100 Ry (the variations of these parameters showed a very low perturbation of the total energies by less than 0.1%). The self-consistent cycles were stopped when variations of the total energy per unit cell and band structure energy were both less than 10^{-4} eV.

3. Results and discussion

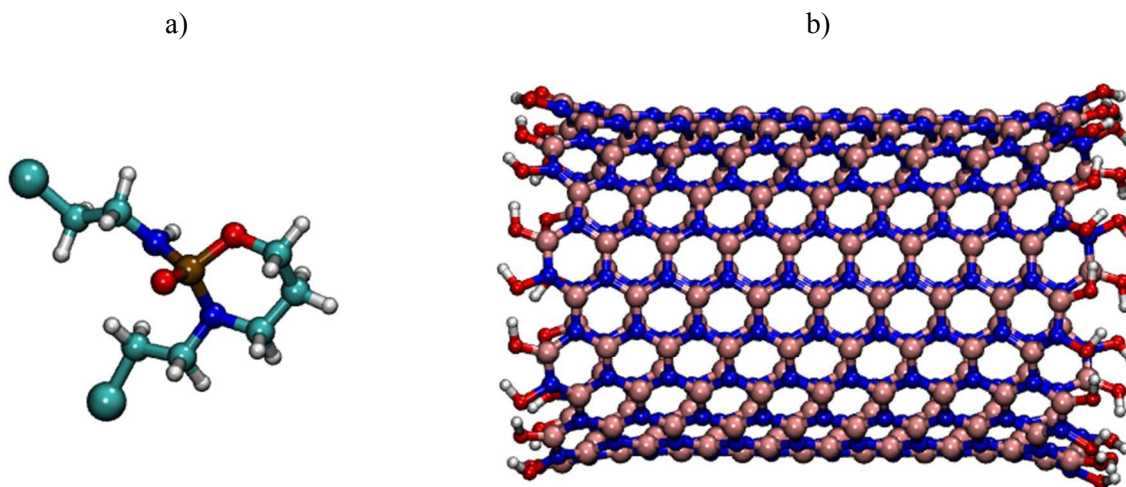


Fig. 1: Geometry of (a) Ifosfamide ($C_7H_{15}Cl_2N_2O_2P$), (b) single-walled (10,10) BNNTs with hydroxyl groups ($-OH$), (B, N, C, O, H, P, and Cl atoms are represented as pink, blue, small cyan, red, white, ochre, large cyan spheres, respectively).

To examine the interaction between the drug molecule and its carrier, we first placed and optimized the Ifos position on the outer surface of the BNNT. The adsorption energy obtained in this configuration was equal to -0.17 eV. While low, it confirms that the Ifos molecule could be stabilized in this position. However, this energy provided by physical interactions (no important charges transfer between the molecule and the BNNT) could not be enough to leave the molecule on the BNNT during its vectorization to the cancer cell.

1
2
3 The investigation of Ifos interaction with the inner surface of BNNT is realized considering the
4 molecule centered along the principal axis of the BNNT. In all simulations, the molecule
5 positions were optimized. The mean distance between the P atom of the molecule and the BNNT
6 center of mass, denoted as d , was calculated for each calculation. Then, the position of the
7 molecule was progressively changed along the tube axis in order to determine the interaction
8 molecule-BNNT with d varying from -21 \AA to 21 \AA . For each distance, the whole structure was
9 relaxed by allowing atom displacement to minimize the total energy. The adsorption energy of
10 the interacting system is obtained by subtracting both the total energy of the isolated tube and the
11 energy of the molecule in gas phase from the total energy of the combined structure after
12 optimization. Fig. 2 shows the adsorption energy of the Ifos molecule as a function of the
13 distance d . As observed in Fig. 2, the interaction presents an asymmetric adsorption energy
14 pathway. We observe a first small energy well around $d = -15 \text{ \AA}$, when the molecule comes close
15 to the nanotube entrance (position (0), Fig. 2). Then a small energy barrier appears (around 40
16 meV of height) which corresponds to the beginning of the molecule encapsulation. It is due to the
17 oxygen and nitrogen atoms hampering the process of encapsulation. Then the molecule
18 experiences a progressive insertion with important negative adsorption energies on the entire
19 pathway (position (1) and thereafter, Fig.2). Between $d = -12 \text{ \AA}$ and $d = 6 \text{ \AA}$, the adsorption
20 energy curve presents a valley with a well around -0.6 eV for $d = 0.0 \text{ \AA}$ (position (2), Fig. 2). It is
21 the most favorable site (close to the geometric center of the nanotube). Note, that the energy
22 slope is less rough after $d = 6 \text{ \AA}$ and until the BNNT edge (i.e. $d = 12 \text{ \AA}$) with an equivalent
23 energetic barrier to the entrance one. We attribute the valley form of adsorption energy at the
24 dissymmetric conformation of the molecule. This can be attributed also to the molecular
25
26
27
28
29
30
31
32
33
34
35
36
37
38
39
40
41
42
43
44
45
46
47
48
49
50
51
52
53
54
55
56
57
58
59
60

geometry, which is slightly tilted compared to the nanotube axis at the beginning and the end of the nanocarrier.

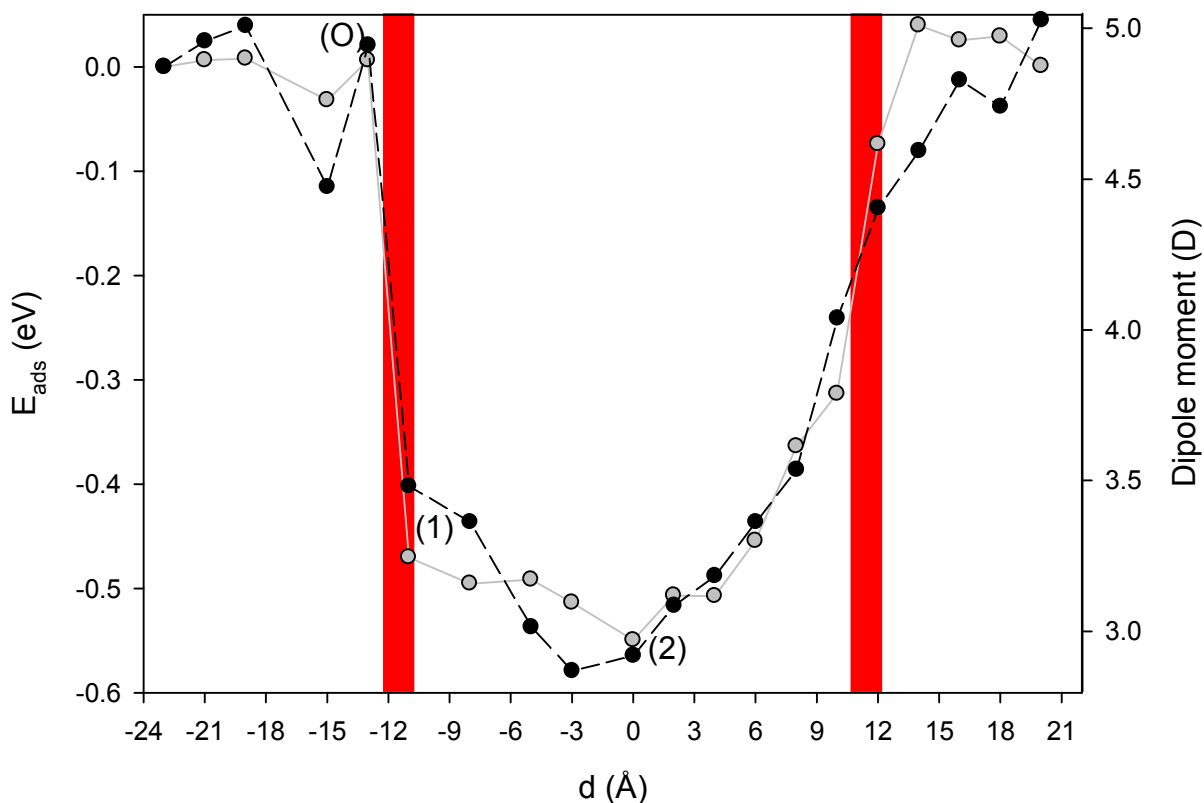


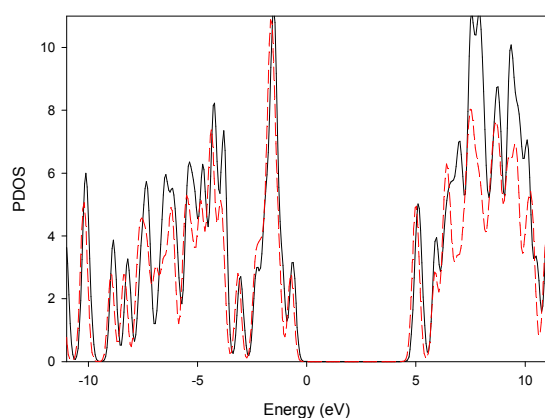
Fig. 2: Interaction energy of Ifos (grey curve) as a function of d , defined as the distance between the absolute position of P atom in the Ifos molecule and the center of mass of BNNT along the z axis. Red bars highlight the BNNT edges. Evolution of the total dipole moment (D) as a function of d (black dashed curve).

In order to have an insight of the interaction between Ifos molecule and the BNNT nanotube, we have sketched the Ifos PDOS molecule for the three most interesting positions (i.e. (O), (1), and (2) labeled on Fig. 2). To facilitate the observation of the evolution, PDOS of Ifos molecule

in gas phase was sketched in red on the different graphs (Fig. 3). In each table associated with the Fig. 3, we have reported the Bader charge evolution onto the different atoms of Ifos molecule and the total electric dipole of the system in Debye, depending on the positions of the molecule (Fig. 3).

Bader Total Charge on isolated Ifos: 84.00 e
Total Dipole on Isolated system: 2.51D -0.91D 4.07D

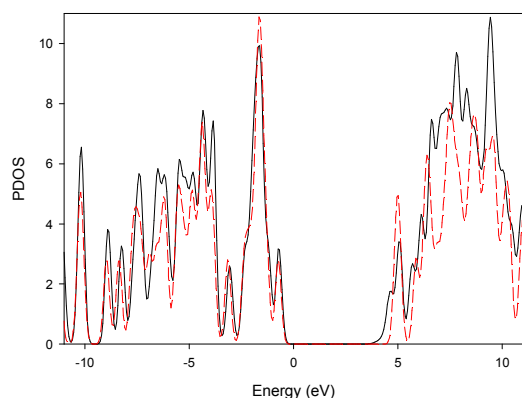
(O)



| Bader charge variation (e) of atom | | | | | |
|---|--------------|-------------|-------------|-------------|-------------|
| P | N | C | O | H | Cl |
| 0.01 | -0.30 | 0.04 | 0.05 | 0.03 | 0.00 |
| Bader Total Charge on Ifos (e) : 84.05 | | | | | |

| Dipole (D) | | |
|-------------|--------------|-------------|
| X | Y | Z |
| 2.13 | -1.82 | 4.10 |

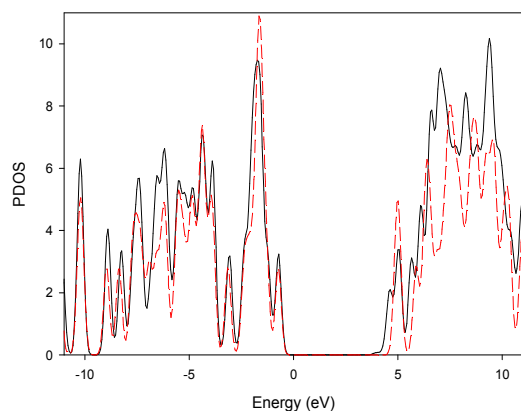
(I)



| Bader charge variation (e) of atom | | | | | |
|---|--------------|--------------|-------------|-------------|--------------|
| P | N | C | O | H | Cl |
| -0.02 | -0.16 | -0.32 | 0.06 | 0.16 | -0.01 |
| Bader Total Charge on Ifos (e) : 83.98 | | | | | |

| Dipole (D) | | |
|-------------|--------------|-------------|
| X | Y | Z |
| 1.97 | -1.23 | 2.59 |

(2)



| Bader charge variation (e) of atom | | | | | |
|---|--------------|-------------|-------------|-------------|-------------|
| P | N | C | O | H | Cl |
| -0.24 | -0.26 | 0.02 | 0.13 | 0.03 | 0.07 |
| Bader Total Charge on Ifos (e) : 84.03 | | | | | |

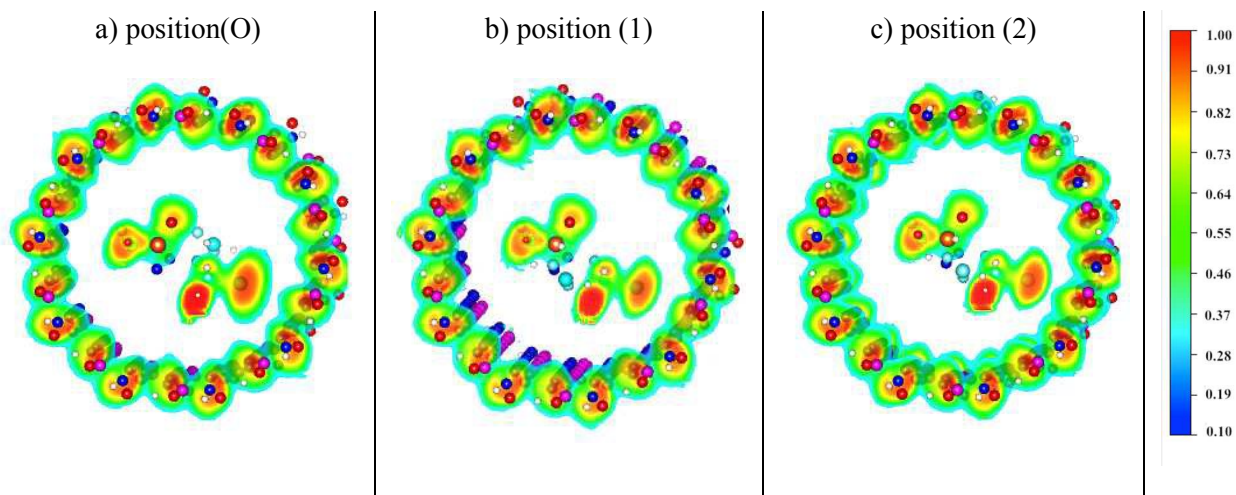
| Dipole (D) | | |
|-------------|--------------|-------------|
| X | Y | Z |
| 2.05 | -0.97 | 1.83 |

Fig. 3: Projected electronic density of states of the Ifos molecule in the three positions depicted in Fig. 2: (O) barrier, (1) well after the entrance of BNNT and (2) most stable site in the BNNT together with those of the molecule in gas phase (red curves). Fermi level was placed at 0 eV. The tables show the mean variations of the Bader charges of the Ifos atoms and the total electric dipole of the system.

The Bader charge evolutions during the Ifos transfer inside the BNNT show some variations for the O, N, C and P atoms with an intra molecular inversion of the variations in function of the position. On the contrary, we observe a weak charge variation on the Cl atoms. The intra charge variation induces a strong variation of the electric dipole of the system between the gas phase and the adsorption positions. The evolution of the dipole moment during the passage of Ifos inside BNNT is characterized by the same behavior than the energy path. It is almost constant (maximum of 0.5D of variation) at the BNNT approach and falls (about 40% of its value) when the molecule comes inside the potential well (Fig. 2, positions 1 and 2). Considering that the encapsulated drug molecules should be ultimately incorporated in human body, the role of the

1
2
3 solvent should be taken into account. Indeed, our DFT calculations did not take into account the
4
5 dispersion repulsion terms and the presence of solvent. However, we have proven recently that
6
7 the role of solvent in BNNT was to stabilize a carboplatin (another anticancer molecule) inside
8
9 the nanocapsules without any event of molecule escape until the end of the simulations and
10
11 the nanocapsules without any event of molecule escape until the end of the simulations and
12
13 concomitant energy value between DFT and all atom molecular dynamic simulation results.²³
14

15
16 To visualize more precisely the physical interactions, we show in Fig. 4 the electron
17
18 localization function (ELF) representation of the system at positions (O) to (2) of Fig. 2. This
19
20 function produces informative patterns and describes chemical bonding in molecules and solids.
21
22 It measures the probability of finding an electron near another electron with the same spin related
23
24 to the Pauli Exclusion Principle.²⁴ The upper limit of the ELF representation corresponds to
25
26 chemical bonding while the values lower than 0.5 correspond to electron-gas-like pair probability
27
28 (i.e. no chemical bonding). As demonstrated in Fig. 4, no chemical interaction was involved in
29
30 the strong confinement of the Ifos inside the BNNT.
31
32
33
34
35
36
37



1
2
3 **Fig. 4:** ELF representation in position (O), (1) and (2) of Fig. 2. The values of each color are
4 depicted in the diagram shown at right. The projection plane sketched is perpendicular to the
5
6
7
8
9
10
11
12
13
14
15
16
17
18
19
20
21
22
23
24
25
26
27
28
29
30
31
32
33
34
35
36
37
38
39
40
41
42
43
44
45
46
47
48
49
50
51
52
53
54
55
56
57
58
59
60

nanotube principal axis and centered onto the P atom. Some atoms are not shown for clarity.

All these data do not show any chemical adsorption or bonding occurring between the molecule and the tube. Moreover, the total Bader charge variation of the Ifos molecule does not exceed 0.05 e, which cannot be attributed to any significant chemical transfer between the molecule and the nanotube.

Note that the role of the chemical saturation of the dangling bonds at the both extremities of the nanotube could influence the energy valley of Ifos. Indeed, it is well known that to increase their dispersion in solvent and developing biomedical applications, two approaches are commonly used. The first one uses covalent attachment of a molecule and the other involves the physical adsorption of a molecular group onto the BNNT surfaces. In the first approach, the most common chemical modification was achieved through the –OH groups at the edges (or defects) of the BNNTs. Nevertheless, H groups can be held on the dangling bonds of nanotubes. To study the influence of this saturation, the energy valley was plotted in Fig. 5 when –H functions saturated the dangling bonds. Small differences are observed. First, the energy barrier at the entrance is translated due to the O atoms lack. Then, the inner position is characterized by a small shift in energy (around 50 meV) that leads to a less stable adsorption site in BNNT saturated with H groups.

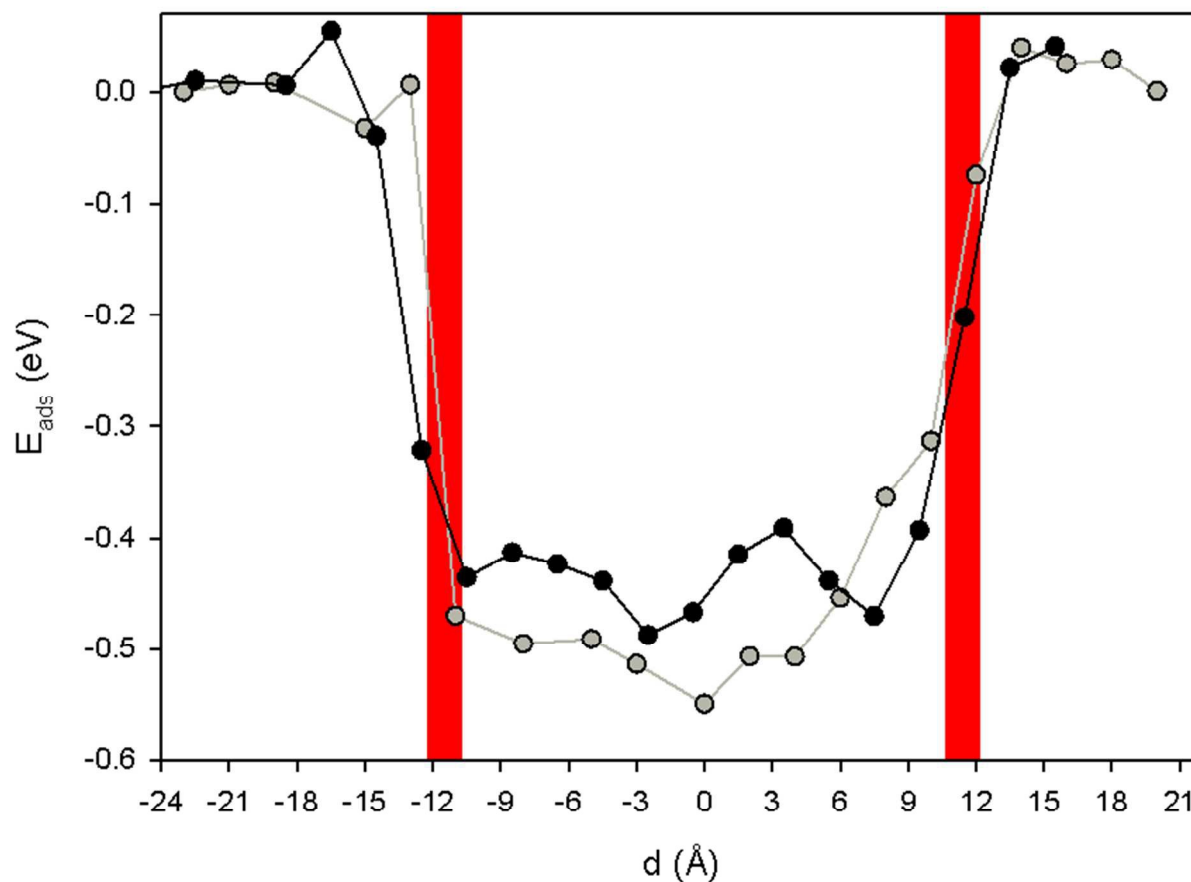


Fig. 5: Interaction energy of Ifos as a function of d for dangling bonds saturated with $-H$ groups (black curve) or with $-OH$ groups (grey curve). Red bars highlight the BNNT edges.

3.4. Discussion

In this study, we show that BNNT could contain inside their internal cavity Ifos molecules. More, we demonstrate with adsorption energy pathway estimated using quantum calculations that BNNT could catch anticancer Ifos molecules spontaneously. The small energy barrier observed at the entrance of the molecule could be crossed easily with thermal agitation at normal temperature. The analysis of the small electronic density of states and charges variations on the

1
2
3 atom constituting the anticancer agents leads to the conclusion that only physical interactions
4
5 were responsible for the molecule and the nanopore surface interaction. This could be explained
6
7 by the low reactivity of the BNNT support. Note that other nanocarriers (such as carbon
8
9 nanotubes) can lead to easy chemical cycloaddition on their surface. The chemical bonds
10
11 obtained between the molecule and its carriers increase the geometric stability of the anticancer
12
13 agent but limit its release near its target unless a specific external excitation arises (infra-red pulse
14
15 for example to break these bonds). In our case, the spontaneous encapsulation of the Ifos could
16
17 prevent the molecule to be released anywhere since its thermodynamic state corresponds to the
18
19 confined position. Indeed, as shown in Fig. 2 the entrance of the BNNT is quite easy to achieve
20
21 (not very high barrier at the entrance, even in the presence of saturated –OH bonds) and the
22
23 molecule falls irremediably into a large potential well (around -0.6 eV). To liberate the toxic
24
25 molecules a third media should be reached (different from BNNT and vacuum) as for example a
26
27 cancer cell if the BNNT outer surface would be functionalized by a specific target function. The
28
29 release of the anticancer drug molecule near the cell should be due to thermal activation in order
30
31 to let interacting the Ifos with the cancer cell. In our case an energy barrier of 0.6 eV should be
32
33 passed to release the anticancer agent. We can note that the energy barrier obtained when the
34
35 dangling bonds are saturated with –H groups is equivalent. Indeed, the small barrier observed in
36
37 this case at the entry of the BNNT is compensated by a lower energy in the inner part of the
38
39 BNNT which leads to the same difference in energy. This energy barrier could be compared to
40
41 the work performed by Panczyck et al.²⁵ who used huge SWCNT as nanocarrier. In this study, the
42
43 release of platinum anticancer agents was extremely rapid (below few minutes) near a cell. The
44
45 estimation of the energy barrier for this release was about 25 kcal/mol (1.08 eV) to compare with
46
47 other experiments developed by Li et al.²⁶ on SWCNT (or Tripisciano et al. on MWCNT²⁷).
48
49
50
51
52
53
54
55
56
57
58
59
60

1
2
3 These latter did not reach such velocity to release drug molecules since 95% of the total
4 encapsulated active molecules near the cancer cell were liberated in 6 hours. The stability of the
5 drug molecule inside the carbon nanocarrier was thus stronger than in our case but the cancer cell
6 presence was sufficient to release the confined molecules. Note that the large discrepancy
7 observed between theoretical and experimental observations could be attributed to structural
8 defects in the carbon structure. Our calculations estimate that the molecules should pass of an
9 energy barrier of only 0.6 eV to exit the BNNT nanotube which tends to facilitate the release of
10 the drug molecule. The residence time of the drug in the BNNT, assuming that the release is
11 thermally active and follows an Arrhenius law, can be estimated to 18 minutes. While extremely
12 low for human life, this could be sufficient at molecular level to transport the drug near its target
13 and deliver the anticancer agent on site. It should be also underlined that contrarily to carbon
14 nanotubes which are ended in equal proportion by zigzag, armchair or chiral structures, the
15 BNNT ended structures are fully dependent on the synthesis methods. BNNTs grown directly
16 from the vapor phase adopted an armchair configuration while those grown from laser-heating
17 and carbon substituted methods are zigzag type. To study the role of the chirality, we have
18 performed some calculations on positions (0), (1) and (2) for a zigzag BNNT saturated by -OH
19 groups. The energies obtained in these positions were slightly different since we obtained
20 0.01eV, -0.44eV and -0.56 eV, for these three positions, respectively. These data show that the
21 Ifos – BNNT interaction are independent of the chirality of the nanocargo.
22
23
24
25
26
27
28
29
30
31
32
33
34
35
36
37
38
39
40
41
42
43
44
45
46
47
48
49

50 **4. Conclusion**

51
52
53 In this study we have investigated the interactions between boron nitride nanotube and
54 anticancer drug ifosfamide using full atoms DFT calculations. Our results show that the
55
56
57
58
59
60

1
2
3 incorporation of Ifos molecules into BNNT does not present any difficulties at room temperature.
4
5 The BNNT nanocarrier represents thus a good candidate for loading this drug and hinders
6
7 premature deactivation of Ifos before reaching the cancer cells. On the contrary of platinum
8
9 agents, Ifos molecules present a large stable potential energy valley in its confined state,
10
11 involving only physical interactions. Indeed, comparison of the density of states of the Ifos
12
13 molecule in the gas phase with the density of states of Ifos incorporated inside BNNT shows
14
15 slight discrepancies only. This particular molecular position protects the anticancer agent from
16
17 any interaction with an external unwanted body and allows the experiments to use the external
18
19 surface area of the nanovector for further chemical functionalization in order to target specifically
20
21 the cancer cells.
22
23
24
25
26
27
28

29 **Acknowledgments**

30
31 This present work was financially supported by University of Franche Comté in its “accueil de
32
33 jeunes chercheurs en séjour de recherche post-doctorale” program.
34
35

36 Calculations were performed with the supercomputer regional facility Mesocenter of the
37
38 University of Franche-Comté.
39
40

41 **References**

- 42
43
44
45
46 (1) Ferrari, M. *Nat. Rev. Cancer* **2005**, *5*, 161-171.
47 (2) Jain, K. K. *Clin. Chem.* **2007**, *53*, 2002-2009.
48 (3) Kim, P. S.; Djazayeri, S.; Zeineldin, R. *Gynecol. Oncol.* **2011**, *120*, 393-403.
49 (4) Kostarelos, K.; Bianco, A.; Prato, M. *Nat. Nano.* **2009**, *4*, 627-633.
50 (5) Bawa, R. *Nanomedicine* **2009**, *5*, 5-7.
51 (6) Liu, Z.; Tabakman, S.; Welsher, K.; Dai, H. *Nano Res.* **2009**, *2*, 85-120.
52 (7) Prato, M.; Kostarelos, K.; Bianco, A. *Acc Chem Res* **2008**, *41*, 60-68.
53 (8) Blase, X.; Rubio, A.; Louie, S. G.; Cohen, M. L. *EPL (Europhysics Letters)* **1994**, *28*, 335.
54 (9) Terao, T.; Zhi, C.; Bando, Y.; Mitome, M.; Tang, C.; Golberg, D. *The Journal of Physical Chemistry C*
55 **2010**, *114*, 4340-4344.
56
57
58
59
60

- 1
2
3 (10) Ciofani, G.; Raffa, V.; Menciacchi, A.; Dario, P. *J. Nanosci. Nanotech.* **2008**, *8*, 6223-6231.
- 4 (11) Ricotti, L.; Fujie, T.; Vazao, H.; Ciofani, G.; Marotta, R.; Brescia, R.; Filippeschi, C.; Corradini, I.;
5 Matteoli, M.; Mattoli, V.; Ferreira, L.; Menciacchi, A. *PLoS ONE* **2013**, *8*, e71707.
- 6 (12) Ciofani, G.; Genchi, G. G.; Liakos, I.; Athanassiou, A.; Dinucci, D.; Chiellini, F.; Mattoli, V. *J Colloid*
7 *Interface Sci* **2012**, *374*, 308-314.
- 8 (13) Sainsbury, T.; Ikuno, T.; Okawa, D.; Pacile, D.; Frechet, J.; Zettl, A.; *The Journal of Physical*
9 *Chemistry C* **2007**, *111*, 12992-12999.
- 10 (14) Zhi, C. Y.; Bando, Y.; Terao, T.; Tang, C. C.; Kuwahara, H.; Golberg, D. *Chemistry – An Asian Journal*
11 **2009**, *4*, 1536-1540.
- 12 (15) Akdim, B.; Kim, S. N.; Naik, R. R.; Maruyama, B.; Pender, M. J.; Pachter, R. *Nanotechnology* **2009**,
13 *20*, 0957-4484.
- 14 (16) Duverger, E.; Gharbi, T.; Delabrousse, E.; Picaud, F. *Phys. Chem. Chem. Phys.* **2014**, *16*, 18425 -
15 18432.
- 16 (17) Ciofani, G.; Danti, S.; Genchi, G. G.; Mazzolai, B.; Mattoli, V. *Small* **2013**, *9*, 1672-1685.
- 17 (18) Ciofani, G.; Danti, S.; Nitti, S.; Mazzolai, B.; Mattoli, V.; Giorgi, M. *Int. J. Pharm.* **2013**, *444*, 85-88.
- 18 (19) Hohenberg, P.; Kohn, W. *Phys. Rev.* **1964**, *136*, B864-B871.
- 19 (20) Kohn, W.; Sham, L. J. *Phys. Rev.* **1965**, *140*, A1133-A1138.
- 20 (21) Perdew, J. P.; Burke, K.; Ernzerhof, M. *Phys. Rev. Lett.* **1996**, *77*, 3865-3868.
- 21 (22) Ordejon, P.; Artacho, E.; Soler, J. M. *Phys. Rev. B* **1996**, *53*, R10441-R10444.
- 22 (23) El Khalifi, M.; Duverger, E.; Gharbi, T.; Boulahdour, H.; Picaud, F. *Physical Chemistry Chemical*
23 *Physics* **2015**, *17*, 30057-30064.
- 24 (24) Silvi, B.; Savin, A. *Nature* **1994**, *371*, 683-689.
- 25 (25) Panczyk, T.; Jagusiak, A.; Pastorin, G.; Ang, W. H.; Narkiewicz-Michalek, J. *J. Phys. Chem. C* **2013**,
26 *117*, 17327-17336.
- 27 (26) Li, J.; Yap, S. Q.; Yoong, S. L.; Nayak, T. R.; Chandra, G. W.; Ang, W. H.; Panczyk, T.; Ramaprabhu,
28 S.; Vashist, S. K.; Sheu, F.-S.; Tan, A.; Pastorin, G. *Carbon* **2012**, *50*, 1625-1634.
- 29 (27) Tripisciano, C.; Kraemer, K.; Taylor, A.; Borowiak-Palen, E. *Chem. Phys. Lett.* **2009**, *478*, 200-205.
- 30
31
32
33
34
35
36
37
38
39
40
41
42
43
44
45
46
47
48
49
50
51
52
53
54
55
56
57
58
59
60

The table of contents:

The encapsulation of phosphorous anti-cancer drugs is spontaneous inside boron nitride nanotube.

